Knowledge-based system for multi-target tracking in a littoral environment

A. Benavoli, L. Chisci *Member, IEEE*, A. Farina, *Fellow, IEEE*,
S. Immediata, L. Timmoneri, G. Zappa

***Abstract*— The paper addresses how to efficiently exploit the *Knowledge-Base (KB)*, e.g. environmental maps and characteristics of the targets, in order to gain improved performance in the tracking of multiple targets via measurements provided by a ship-borne radar operating in a littoral environment. In this scenario, the non homogeneity of the surveillance region makes the *conventional* tracking systems (not using the KB) very sensitive to false alarms and/or missed detections. It will be demonstrated that an effective use of the KB can be exploited at various levels of the tracking algorithms so as to significantly reduce the number of false alarms, missed detections, false tracks and improve true target track life. The KB will be exploited at two different levels. First, some key parameters of the tracking system are made dependent upon the track location, e.g., sea, land, coast, *meteo* zones (i.e. zones affected by meteorological phenomena) etc.. Secondly, modifications are introduced to cope with a priori identified regions with high clutter density (e.g. littoral areas, roads, meteo zones etc.). To evaluate the behavior of the proposed knowledge-based tracking systems, extensive results will be presented using both simulated and real radar data.**

***Index Terms*— Multiple target tracking; knowledge-based systems; data association; interacting multiple models; Kalman filtering.**

I. INTRODUCTION

THE paper deals with multi-target tracking using a ship-borne radar system. This system is required to operate in a challenging environment crowded with non intentional interference (sea clutter, littoral clutter and ground clutter), intentional interference (jammers) and in presence of commercial and military air and naval targets; in addition to this, other targets exist, like vehicular traffic, that may confuse the radar. The aim of the work is the development of a *Knowledge-Based Tracker (KBT)* that, exploiting environmental maps as well as information on the characteristics of the targets, is able to

1) reduce the number of false tracks;
2) speedup and make more efficient the initiation of true (target) tracks;
3) improve the life of true tracks.

The KBT attains these goals by combining the information coming from the radar sensor (e.g. echoes from targets and clutter) with the contextual information (e.g. geographic, meteo (*meteorological*), clutter and road maps as well as target characteristics). The architecture of the tracking system must take into account the environment where the radar system is operating, which is characterized by the presence of multiple targets with different kinematic behaviors. To this end, the *Extended Kalman Filter (EKF)* allows the design of a filter for each type of target that can be present in the environment, while the selection of the appropriate filter for each target can be managed by the *Interacting Multiple Model (IMM)* [5].

Another key problem in radar tracking is data association, i.e. the assignment of plots to tracks. There exist a wide range of techniques including NN (*Nearest Neighbor*), PDA (*Probabilistic Data Association*), JPDA (*Joint Probabilistic Data Association*), MHT (*Multiple Hypothesis Tracking*). Although the NN algorithm is still widely used and attractive for its low computational requirements, a global optimum approach (e.g. JPDA) is certainly preferable in a multi-target scenario. Since global optimum approaches are too computationally expensive, a sub-optimal technique known as NNCJPDA (*NN Cheap JPDA*) [9, ch. 1] is adopted in this work.

Another task to be accomplished by the tracking system is the initiation/termination of tracks that has been implemented using the well known M/N logic [14].

A KBT [15],[16] is realized by integrating the filtering, association and track formation procedures with the available *Knowledge-Base* (KB). In particular the KBT proposed in this work will accomplish this integration by:

- tuning some key parameters of the filtering, association and track formation algorithms;
- introducing appropriate strategies for the management of the critical (high-density clutter) zones of the surveillance environment.

Two specific strategies are devised to cope with high-clutter regions: a first strategy eliminates all measurements falling inside such regions and exhibits a good behavior except for the case in which the target is maneuvering in such regions; a second strategy preserves all measurements and eliminates the tracks *persisting* in the high clutter regions. As a further contribution, this paper will analyze the potential benefits arising from the exploitation of the target amplitude provided by the radar sensor. It is well known that the amplitude of the echo may help in the discrimination among useful target returns and reflections of the environment surrounding the radar. In particular, the advantage of using the amplitude information in the data association will be evaluated.

The rest of the paper is organized as follows. Section 2 reviews the basic building blocks of a modern multi-target tracking system and presents the architecture of the tracker

Authors' addresses:
A. Benavoli, *L. Chisci* and *G. Zappa*, DSI, Università di Firenze, Firenze, Italy, e-mail: $\{benavoli,\ chisci\}$@dsi.unifi.it;
A. Farina, *S. Immediata* and *L. Timmoneri*, Engineering Division, SELEX - Sistemi Integrati S.p.A., Rome, Italy, e-mail: $\{afarina,\ simmediata,\ ltimmoneri\}$@selex-si.com.

considered in this work, including the design of the filter bank and the selection of the data association logic. Section 3 details the proposed KBT approach and its application to multi-target tracking in a littoral environment, while Section 4 discusses the results obtained on simulated and live data relative to one of the AMS (Alenia Marconi Systems) naval surveillance systems. Finally, Section 5 concludes the paper.

II. Architecture of the tracking filter

Target tracking from radar observations is a difficult task, because of false alarms and of the simultaneous presence of multiple targets with *detection probability* $P_d < 1$. At each scan, the radar provides a set $Z(k) = \{\mathbf{z}_i(k) = [r_i(k), \theta_i(k)] : i = 1, 2, \ldots, m(k)\}$ of position measurements in polar coordinates (range and azimuth) w.r.t. the radar position. These measurements are employed by the tracking system to perform three main tasks [1]:

- **filtering**, i.e. the update of the target state using measurements and a model of the target motion;
- **data association**, i.e. the association of measurements to already established tracks;
- **track initiation**, i.e. the detection of the presence of new targets in the surveillance area.

A. Filtering

The filtering task consists of estimating the kinematic variables (e.g., positions, velocities, etc.) of the target using measurements and a model of the target motion. The basic tool employed for this is the *Kalman Filter (KF)*, whenever the model is linear, or its linearization around the current estimate, called *Extended Kalman Filter (EKF)*, when the model is nonlinear. Unfortunately, it is well known [8] that a single-model filter is inadequate for tracking targets with fast maneuvering capabilities (e.g., helicopters or military aircrafts). To this end, *Multiple Model (MM)* filters have been proposed in order to provide a greater flexibility in modelling different behaviors of the target. In fact, MM algorithms use a bank of filters each of which is based on a specific model tailored to a possible target behavior (e.g. straight line motion, left turn, right turn etc.). There exist a large variety of MM algorithms [2] depending on the *model set selection* as well as on the type of interaction between the filters (e.g. *SMM: Static Multiple Model* [2]; *GPB: Generalized Pseudo-Bayesian* [3], [4]; *IMM: Interacting Multiple Model* [5]; *VS-IMM: Variable Structure IMM* [2]). In order to cope with frequent and sudden maneuvers of the target, the so called *Interacting Multiple Model (IMM)* approach has been adopted in this work. This choice has been motivated by the observation, after extensive computer simulations, that IMM provides an optimal trade-off between on-line computational burden and tracking performance.

Let $\mathcal{M} = \{\mathcal{M}_1, \mathcal{M}_2, \ldots, \mathcal{M}_\mu\}$ denote the model set where each model $\mathcal{M}_i$ is of the form:

$$\mathcal{M}_i : \left\{ \begin{array}{rcl} \mathbf{x}(k+1) & = & \mathbf{f}_i(\mathbf{x}(k)) + \mathbf{w}_i(k) \\ \mathbf{z}(k) & = & \mathbf{h}(\mathbf{x}(k)) + \mathbf{v}(k) \end{array} \right. \quad (1)$$

where: $\mathbf{x}$ is the target state; $\mathbf{z}$ is the target measurement; $\mathbf{w}_i$ and $\mathbf{v}$ are the process and the measurement noise, respectively. In the IMM filter, the transition mechanism between the various models $\mathcal{M}_i$ is described by a *homogeneous Markov chain* wherein the probabilities of transition from model $\mathcal{M}_i$ to model $\mathcal{M}_j$ are assumed constant and equal to a priori given values π_{ij}. For the sake of completeness, a full cycle of the IMM tracking filter is summarized in Table I: the reader can refer to [2] for details. The degrees of freedom in the IMM filter are the a priori model transition probabilities π_{ij} and, most importantly, the model set $\mathcal{M}$. In particular the choice of the model set is of vital importance and must trade-off computational load (i.e. low μ), on one hand, and target modelling flexibility (i.e. high μ) on the other. A variety of models has been proposed in the literature (e.g. Singer model [6], constant velocity model, coordinated turn models [8], etc.) to describe different kinematic behaviors of the target. In particular, *Coordinated Turn (CT)* models have been found especially useful in this work in order to provide a satisfactory description of the motion for all targets of interest (e.g., ships, helicopters, civil and military aircrafts) with a limited number of models (just three), thus implying an acceptable on-line computational burden.

Consider the target state vector $\mathbf{x} = [x,\ y,\ v,\ h]'$ where x, y are the cartesian coordinates of the target position, v is the speed modulus and h is the heading angle. Further, consider the following nonlinear state equations:

$$\begin{bmatrix} x^+ \\ y^+ \\ v^+ \\ h^+ \end{bmatrix} = \begin{bmatrix} x + \frac{2}{\omega_0} v\ sin\left(\frac{\omega_0 T}{2}\right)\ cos\left(h + \frac{\omega_0 T}{2}\right) \\ y + \frac{2}{\omega_0} v\ sin\left(\frac{\omega_0 T}{2}\right)\ sin\left(h + \frac{\omega_0 T}{2}\right) \\ v \\ h + \omega_0 T \end{bmatrix} + \mathbf{w} \quad (2)$$

where: T is the scan period; x, y, v, h denote the state variables at scan k; x^+, y^+, v^+, h^+ are the state variables at scan $k+1$; $\mathbf{w} = \mathbf{w}(k)$ is the process disturbance, assumed zero mean and with covariance $\mathbf{Q} = diag\{0, 0, T\sigma_v^2, T\sigma_h^2\}$. Notice that in (2) the angular speed $\omega = \dot{h}$ has been considered as a fixed parameter ω_0. In fact, the inclusion of the angular speed ω in the state vector and its estimation are not convenient for short-duration maneuvers (e.g., military aircraft or helicopter) since there is little time for a reliable estimation of ω. For $\omega_0 = 0$ the model (2) describes a motion with constant velocity and constant heading (straight motion). Conversely for $\omega_0 \neq 0$ it describes a maneuver (*turn*) with constant angular speed ω_0, a *left turn* ($\omega_0 > 0$) or a *right turn* ($\omega_0 < 0$) depending on the sign of ω_0. It has been found that the following three models:

1) *Constant Velocity (CV)* model (2) obtained for $\omega_0 = 0$,
2) *Left Coordinated Turn (CT_+)* model (2) obtained for $\omega_0 > 0$,
3) *Right Coordinated Turn (CT_-)* model (2) obtained for $\omega_0 < 0$,

provide an adequate and self-contained model set for our tracking purposes. Hence, the model set for IMM has been selected as follows:

$$\mu = 3, \quad \mathcal{M}_1 = CV, \quad \mathcal{M}_2 = CT_+, \quad \mathcal{M}_3 = CT_-$$

Notice that all the three models have the same state variables; this greatly simplifies the re-initialization and fusion

operations of the IMM filter. The state equation (2) must be paired with the output (measurement) equation that, obviously, is common to all the models and turns out to be:

$$\mathbf{z} \;=\; \left[\begin{array}{c} \sqrt{x^2+y^2} \\ \angle(x+jy) \end{array} \right] \;+\; \mathbf{v}$$

where $\mathbf{v} = \mathbf{v}(k)$ is the measurement noise, assumed zero mean and with covariance $\mathbf{R} = diag\{\sigma_r^2, \sigma_\theta^2\}$. Since the models (both the state and the output equations) are nonlinear, the IMM filter requires a bank of three EKFs for the models CV, CT_+ and CT_-.

B. Data association

Data association aims at assigning a given set of measurements (plots) to a given set of tracks. There exist a great deal of data association techniques in the literature [7]. A first classification is among *single-target* and *multi-target* techniques. The former proceed track-by-track in the association so that when a given track is considered, the presence of the other tracks is ignored. Conversely, *multi-target* techniques carry out the association procedure jointly for all tracks so that multiple (nearby) targets actually compete for the same measurements. A second important distinction is among *soft-decision* and *hard-decision* techniques. Soft-decision techniques do not select a specific measurement for a given track, but update the track's state with a combination of all measurements suitably weighted by their association probabilities. Conversely, hard-decision techniques associate to each track at most a single measurement, selected as the one maximizing the association probability. Another relevant distinction is among *single-scan* and *multi-scan* techniques. The former only consider the measurements at the present scan while the latter also consider measurements collected over a given number of past scans in order to remedy possible previous association errors [11]-[13].

The choice of an appropriate data association algorithm for radar tracking in a coastal environment must take into account the following two features.

1) There can be multiple, possibly nearby, targets within the radar surveillance area.
2) The number of targets is not fixed a priori and a new target can enter the surveillance area at any time.

To cope with the above two difficulties and also to limit the computational complexity, a *multi-target hard-decision single-scan* data association algorithm is preferable. Let $Z = \{\mathbf{z}_1, \mathbf{z}_2, \ldots, \mathbf{z}_m\}$ and $\mathcal{T} = \{\tau_1, \tau_2, \ldots, \tau_n\}$ denote the set of measurements and, respectively, the set of tracks to be associated at a given scan. For data association purposes, each track is represented by a pair $\tau_j = (\hat{\mathbf{z}}_j, \mathbf{S}_j)$ where $\hat{\mathbf{z}}_j$ is the measurement prediction and $\mathbf{S}_j$ the prediction error covariance, that are both updated via a tracking filter as described in subsection 2.1. Hence, a multitarget hard-decision single-scan association is a relation $\mathcal{A} \subseteq \{1, 2, \ldots, m\} \times \{1, 2, \ldots, n\}$ such that

- each measurement $\mathbf{z}_i$ is associated to at most one track;
- at most one measurement is associated to each track τ_j.

The specific data association algorithm adopted in this work is the so called *NNCJPDA (Nearest Neighbor Cheap Joint Probabilistic Data Association)* [9, ch. 1] as it provides a good trade-off between on-line computational burden and performance in terms of low probability of wrong associations. Let $\mathcal{N}(\mathbf{z}; \hat{\mathbf{z}}, \mathbf{S}) \triangleq det(2\pi\mathbf{S})^{-1}\; e^{-\frac{1}{2}(\mathbf{z}-\hat{\mathbf{z}})'\mathbf{S}^{-1}(\mathbf{z}-\hat{\mathbf{z}})}$ denote the gaussian pdf with mean $\hat{\mathbf{z}}$ and covariance $\mathbf{S}$ and

$$\mathcal{E}(\hat{\mathbf{z}}, \mathbf{S}, \gamma) \triangleq \{\mathbf{z} : (\mathbf{z}-\hat{\mathbf{z}})'\mathbf{S}^{-1}(\mathbf{z}-\hat{\mathbf{z}}) \le \gamma\} \tag{3}$$

denote the corresponding *confidence ellipsoid* with *gating probability* $P_g = Prob(\ \mathbf{z} \in \mathcal{E}(\hat{\mathbf{z}}, \mathbf{S}, \gamma)\ )$, related to $\gamma > 0$ via the χ^2 distribution. Then the NNCJPDA algorithm operates as follows.

1) For all pairs $(i, j) \in \{1, 2, \ldots, m\} \times \{1, 2, \ldots, n\}$ compute the probability β_{ij} of associating measurement $\mathbf{z}_i$ to track τ_j by

$$\beta_{ij} \;=\; \frac{e_{ij}}{\sum_{k=1}^{n} e_{ik} + \sum_{k=1}^{m} e_{kj} \;- e_{ij} + b} \tag{4}$$

where

$$e_{ij} \;=\; \left\{ \begin{array}{ll} 0, & \mathbf{z}_i \notin \mathcal{E}(\hat{\mathbf{z}}_j, \mathbf{S}_j, \gamma) \\ \mathcal{N}(\mathbf{z}_i; \hat{\mathbf{z}}_j, \mathbf{S}_j), & \mathbf{z}_i \in \mathcal{E}(\hat{\mathbf{z}}_j, \mathbf{S}_j, \gamma) \end{array} \right. \tag{5}$$

and $\gamma > 0,\ b > 0$ are suitably chosen parameters.
2) Set $\mathcal{L} = \{(i, j) :\ \beta_{ij} > 0\}$ and $\mathcal{A} = \emptyset$.
3) Repeat the following steps until $\mathcal{L}$ is empty:

$$(i^*, j^*) \;=\; \arg \max_{(i,j)\in\mathcal{L}} \beta_{ij} \tag{6}$$

$$\mathcal{A} \;=\; \mathcal{A} \cup (i^*, j^*) \tag{7}$$

$$\mathcal{L} \;=\; \mathcal{L} \setminus \{(i, j) : i = i^* \text{ or } j = j^*\} \tag{8}$$

Notice that at the end of the above procedure there can be tracks τ_j with no associated measurements (*missed detections*). Moreover there can also be measurements $\mathbf{z}_i$ not associated to any track; such measurements can be passed to another set of lower priority tracks for a further data association round or can initiate new tracks (see the next subsection on track initiation). A few remarks on the NNCJPDA algorithm are in order.

- The equations (4)-(5) provide a computationally *cheap* and approximate evaluation of the true association probabilities (CJPDA). CJPDA has been employed, in place of the exact JPDA [7, ch. 6],[10] since it implies a significantly lower computational load and also provides a satisfactory association performance.
- A null association probability is assigned by (5) whenever the measurement $\mathbf{z}_i$ falls outside the validation region $\mathcal{E}(\hat{\mathbf{z}}_j, \mathbf{S}_j, \gamma)$ of the track τ_j. In this way only measurements that lie inside the ellipsoid $\mathcal{E}(\hat{\mathbf{z}}_j, \mathbf{S}_j, \gamma)$ can be assigned to the track τ_j. Clearly $\gamma > 0$, or equivalently the related *gating probability* P_g, tunes the size of the validation region and is, therefore, a parameter of paramount importance in the association algorithm. Another key parameter is $b > 0$ which, according to (4), accounts for both the probability of missed detection and

TABLE I
ONE CYCLE OF THE IMM FILTER

1. **Re-initialization** (for $j = 1, 2, \ldots, \mu$):

Predicted model probability:
$$p_j(k|k-1) \;=\; \sum_{i=1}^{\mu} \pi_{ij}\; p_i(k-1)$$
Mixing probabilities:
$$p_{i|j}(k-1) \;=\; \frac{\pi_{ij}\; p_i(k-1)}{p_j(k|k-1)}$$
Mixing estimate:
$$\overline{x}_j(k-1|k-1) \;=\; \sum_{i=1}^{\mu} p_{i|j}(k-1)\; \hat{x}_i(k-1|k-1)$$
Mixing covariance:
$$\overline{P}_j(k-1|k-1) \;=\; \sum_{i=1}^{\mu} p_{i|j}(k-1)\; \left[P_i(k-1|k-1) + \left(\overline{x}_j(k-1|k-1) - \hat{x}_i(k-1|k-1)\right)\left(\overline{x}_j(k-1|k-1) - \hat{x}_i(k-1|k-1)\right)'\right]$$

2. **Update of the filter bank** (for $j = 1, 2, \ldots, \mu$):

Model linearization:
$$F_j(k) = \left[\frac{\partial f(\cdot)}{\partial x}\right]_{x=\overline{x}_j(k-1|k-1)} \qquad H_j(k) = \left[\frac{\partial h(\cdot)}{\partial x}\right]_{x=\hat{x}_j(k|k-1)}$$
Predicted state:
$$\hat{x}_j(k|k-1) \;=\; f_j\left(k-1,\; \overline{x}_j(k-1|k-1)\right)$$
Predicted covariance:
$$\hat{P}_j(k|k-1) \;=\; F_j(k-1)\; \overline{P}_j(k-1|k-1)\; F_j'(k-1) \;+\; Q_j(k-1)$$
Measurement residual:
$$\tilde{z}_j(k) \;=\; z(k) - h(k, \hat{x}_j(k|k-1))$$
Residual covariance:
$$S_j(k) \;=\; H_j(k)\; P_j(k|k-1)\; H_j'(k) \;+\; R_j(k)$$
Filter gain:
$$K_j(k) \;=\; P_j(k|k-1)\; H_j'(k)\; S_j^{-1}(k))$$
Update state:
$$\hat{x}_j(k|k) \;=\; \hat{x}_j(k|k-1) \;+\; K_j(k)\; \tilde{z}_j(k)$$
Update covariance:
$$P_j(k|k) \;=\; P_j(k|k-1) \;-\; K_j(k)\; S_j(k)\; K_j'(k)$$

3. **Model probability update** (for $j = 1, 2, \ldots, \mu$):

Model likelihood:
$$L_j(k) \;=\; \mathcal{N}\left(\tilde{z}_j(k); 0, S_j(k)\right)$$
Model probability:
$$p_j(k) \;=\; \frac{p_j(k|k-1)\; L_j(k)}{\sum_{i=1}^{\mu} p_i(k|k-1)\; L_i(k)}$$

4. **Estimate fusion:**

Overall estimate:
$$\hat{x}(k|k) \;=\; \sum_{i=1}^{\mu} p_i(k)\; \hat{x}_i(k|k)$$
Overall covariance:
$$P(k/k) \;=\; \sum_{i=1}^{\mu} p_i(k)\; [P_i(k/k) \;+\; (\hat{x}(k|k) - \hat{x}_i(k|k))(\hat{x}(k|k) - \hat{x}_i(k|k))']$$

the probability of wrong association. The parameter b is related to the *false alarm probability* P_{fa} by

$$b = \frac{P_{fa}}{A_{rc}}\; \frac{1 - P_d P_g}{P_g} \tag{9}$$

where A_{rc} is the area of the radar cell.

- If the above data association algorithm is used in conjunction with an IMM tracking filter that actually provides, for a given track, μ prediction-covariance pairs corresponding to the different models $\mathcal{M}_\ell$, a partial association probability $\beta_{ij}^{(\ell)}$ is evaluated for each model $\mathcal{M}_\ell$ and then an overall association probability β_{ij} is obtained by combining the partial association probabilities with the model probabilities p_ℓ provided by the IMM, i.e.

$$\beta_{ij} \;=\; \sum_{\ell=1}^{\mu} p_\ell\; \beta_{ij}^{(\ell)}$$

C. Track initiation

The logic of initiation/promotion/termination of tracks is described by the state diagram of Figure 1. Notice that *new*, *tentative* and *confirmed* tracks have different priorities in the *data association* (see fig 3). In fact *confirmed tracks* get, at each scan k, the whole set of measurements $Z(k)$ while *tentative tracks* get only the subset of measurements $Z_{nc}(k)$ that have been discarded by confirmed tracks and *new tracks* get the subset of measurements $Z_{nt}(k) \subset Z_{nc}(k)$ that have been discarded by tentative tracks. Further, let $Z_{nn}(k) \subset Z_{nt}(k)$ denote the subset of measurements that are not associated to any existing track, then any measurement in $Z_{nn}(k)$ initiates a *new track* at scan $k+1$. The promotion of a track from *new* to *tentative*, at scan k, requires a pair of measurements $\mathbf{z}(k-1) = [r(k-1), \theta(k-1)]' \in Z_{nn}(k-1)$ and $\mathbf{z}(k) = [r(k), \theta(k)]' \in Z_{nc}(k)$ that satisfy the following gating condition:

$$\left|\; r(k)\; e^{j\theta(k)} - r(k-1)\; e^{j\theta(k-1)} \;\right| \;\leq\; v_{max} T \tag{10}$$

where v_{max} is the maximum speed of a target and T is the scan period. Clearly (10) amounts to requiring that the distance of the two positions is not greater than $v_{max}T$. A *new track* that fails to meet the condition (10) for some $\mathbf{z}(k) \in Z_{nc}(k)$ is immediately terminated. Conversely, whenever (10) is satisfied, a tracking filter for the *tentative track* is initialized in order to provide, at subsequent scans $i > k$, the track prediction $\hat{z}(i) \stackrel{\triangle}{=} \hat{z}(i|i-1)$ required for data association. A simpler EKF based on a (single) CV model is used for *tentative tracks* in place of the computationally more demanding IMM-filter adopted for *confirmed tracks*; notice that this implies a considerable saving of computational power as the tentative tracks are by far more numerous than the confirmed tracks.

The initial state of this filter is, therefore, set equal to

$$\begin{cases} x(k) &= r(k)\ sin\ \theta(k) \\ y(k) &= r(k)\ cos\ \theta(k) \\ v(k) &= \sqrt{\left(\frac{x(k)-x(k-1)}{T}\right)^2 + \left(\frac{y(k)-y(k-1)}{T}\right)^2} \\ h(k) &= \angle\left(x(k)-x(k-1)\right) + j\left(y(k)-y(k-1)\right) \end{cases} \tag{11}$$

A *tentative track* undergoes, at each scan, the data association procedure described in the previous section and the update of the associated tracking filter. The data association can have two possible outcomes for a given track: either a successful plot association or a missed plot. The promotion from *tentative* to *confirmed* track is ruled by the well known *M/N logic* [1], [14]. Two integer parameters M and N such that $1 \leq M < N$ are chosen; then the tentative track is *confirmed* if the number of plots over N consecutive scans is at least M, otherwise the track is terminated. The choice of M and N must be related to the target detection probability P_d as well as to the false alarm probability P_{fa}; for instance, reasonable values should satisfy the following constraints

$$A_{vr}P_{fa} \ \leq\ \frac{M}{N}\ \leq\ P_d \tag{12}$$

where A_{vr} is the average area of the validation region. A confirmed track is terminated whenever it goes through L consecutive missed detections (see Figure 1).

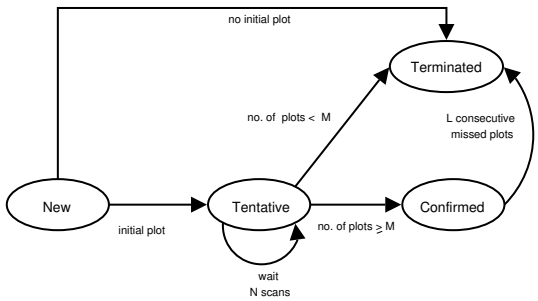

Fig. 1. M/N logic

III. KNOWLEDGE-BASED TRACKER

A major problem in target tracking is the ambiguity on the source of a measurement; in fact a radar measurement can be produced either from a target (ship, aircraft, helicopter) or from clutter. In the scenario considered in this work, i.e. a ship-borne radar operating in a littoral environment, clutter echoes are mainly due to mountains, shores, buildings, but also vehicles on roads, highways and railways. The sources of the clutter are located in specific points of the surveillance environment so that the clutter density is not uniform, as shown in Figure 2. Hence it is convenient to divide the surveillance region into zones of three types according to their

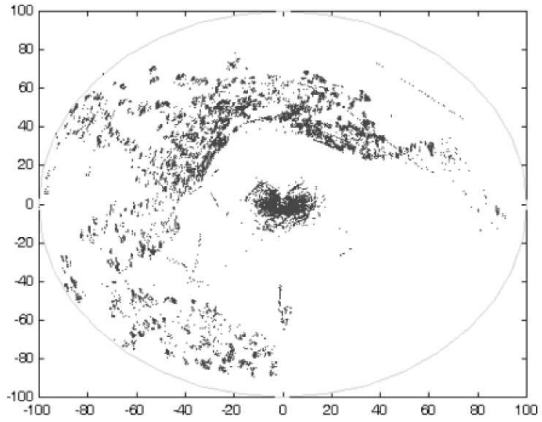

Fig. 2. Clutter map

clutter density, viz.

1. Low Clutter (LC) zones $(P_{fa} < P_{fa}^1)$,
2. Medium Clutter (MC) zones $(P_{fa}^1 \leq P_{fa} \leq P_{fa}^2)$,
3. High Clutter (HC) zones $(P_{fa} > P_{fa}^2)$.

(13)

where the threshold values P_{fa}^1 and P_{fa}^2 of the false alarm probability are design parameters to be properly tuned so as to meet the desired specification in terms of number of false tracks confirmed per hour. LC zones are typically the sea and shadowed areas. MC zones are the ground and meteo zones. Finally HC zones can be classified into two types: small-extension HC zones like towns, roads, highways and railways and large-extension HC zones like shores and mountains.
Clutter sources are troublesome as they generate false measurements and this can:

- cause errors in track initiation, with the consequent formation of false tracks;
- cause errors in data association, with the consequent loss of target tracks;
- prevent the termination of false tracks in the HC zones, wherein such tracks are very likely to be updated with clutter measurements.

To prevent such problems, the idea pursued in this work is to use the prior knowledge of the clutter distribution in order to improve the performance of the tracking system described in the previous section [15]-[16]. In fact, since the clutter density depends on the characteristic of a given zone (e.g. sea, ground, meteo zones, etc.), it is possible to use

- the environmental map,
- the meteorological map,
- the road map,
- the clutter map,

of the surveillance region so as to check if the source of a given measurement is in an LC, MC or HC zone and, accordingly,

adopt different strategies in the three cases. These maps, along with the information about the targets to be discussed later, form the so called *Knowledge-Base (KB)*. The target tracking algorithm which exploits the KB will be referred as KB Tracker (KBT). Figure 3 shows the architecture of the tracking system presented in Section II and illustrates how the KB can be included in this architecture. In particular it can be observed that:

- *new*, *tentative* and *confirmed* tracks have different priorities in the *data association*;
- *tentative* and *confirmed* tracks use two different filtering algorithms, respectively EKF and IMM;
- the KB utilizes the environmental maps and the information about the targets.

A key problem is how to fuse the various maps in order to suitably partition the surveillance region into LC, MC and HC zones. The main concern has been to avoid possible misclassifications of high (respectively medium) as medium (respectively low) clutter zones. To this end, a worst-case approach has been pursued i.e. a clutter zone has been classified as LC, MC or HC according to the highest clutter density encountered among the available maps. In the classification, it is also important to take into account the measurement errors that can produce the above-mentioned misclassifications and hence a faulty behavior of the KBT system. To prevent this, the clutter zones have been widened according to the standard deviation of the radar measurement error.

A. Application of the KB to the tracking system

The first application of the KB to the tracking algorithm consists of tuning some parameters of the data association and track initiation algorithms according to the track location in an LC, MC or HC zone. In fact, as these parameters depend on the clutter density, it is natural to adapt them according to the track position on the maps.
In particular, the parameters managed according to the KB are the following:

- M, N for track initiation (M/N logic),
- b for data association,
- γ for the validation ellipse.

These parameters - as can be seen in (3), (9) and (12) - depend on the false alarm probability P_{fa} and on the detection probability P_d. The knowledge-based parameter tuning must take into account two conflicting aims: *(1) to maximize the probability of true target tracking* P_{TTT} and *(2) to maximize the probability of false track rejection* P_{FTR}. For example, as far as the choice of M and N is concerned, the first aim requires to select low values for M and N, while the second calls for high values. The designer must, therefore, select the parameters according to the specifications (P_{TTT} and P_{FTR}) on the performance of the tracking system, and also according to the location of the track on the maps that, clearly, affects the value of P_{fa} and, in turn, must affect the parameters choices. Table II reports the specific zone-dependent choices of the parameters M, N, b, γ adopted in this paper to design the KBT (other parameters L and L_s to be defined later are also reported).

The zone-dependence of the above parameters, unfortunately, is not enough to provide good tracking performance in HC zones. To this end, two strategies have been devised:

1) **DMHC** (*Delete Measurements in High Clutter* zones),
2) **DTPHC** (*Delete Tracks Persisting in High Clutter* zones).

B. DMHC

The DMHC strategy consists of deleting all measurements in the HC zones, before they are processed by the tracking algorithm. To accomplish this task, the KB is used. Unfortunately the deleted areas create artificial shadow zones and, therefore, enforce missed detections for the tracks crossing HC zones. Hence, in order to prevent unmotivated terminations of such tracks, the idea is to increase the parameter L (number of consecutive missed plots for the termination of a confirmed track) in the HC zones. Figure 4 depicts the two tasks of the DMHC strategy, i.e

- the elimination, from the radar measurement set Z, of the measurements located in the HC zones (via the *Measurements filter* block);
- the increase, for the tracks in the HC zones, of the parameter L.

C. DTPHC

The DTPHC strategy affects the tracking algorithm in the following three tasks:

- it prevents the initiation of *new* tracks in the HC zones;
- it does not confirm *tentative* tracks that persist for several scans in the HC zones;
- it deletes *confirmed* tracks that have persisted in HC zones for a sufficiently high number of consecutive scans.

A track is classified as *persistent* in a HC zone whenever it stays in such a zone for L_s consecutive scans. The integer L_s is, therefore, a key parameter of the DTPHC strategy. The idea underlying the DTPHC approach is that a track persisting for a long time in a HC zone is very likely to be false. For example, along a road or highway there can be many false tracks due to motor vehicles. These tracks, clearly, move along the road/highway (HC zone) and, thus, are easily recognized as false and terminated. The DTPHC strategy is illustrated in Figure 5. In particular it can be observed as this strategy manages the promotion/maintenance/termination of the tracks in the HC zones.

D. Target classification

The classification of the target type (ship, civil aircraft, military aircraft, helicopter, etc.) is an important task of target tracking. Performing target classification can provide an improvement in the system performance. In fact, since the targets of interest have different characteristics of speed and maneuverability, it is possible to exploit such differences to fit the tracking algorithms to the target type. To classify the target, one can exploit the a priori information on the target characteristics as well as the environmental maps (that are part of the KB) by means of a set of rules. Typical rules based on

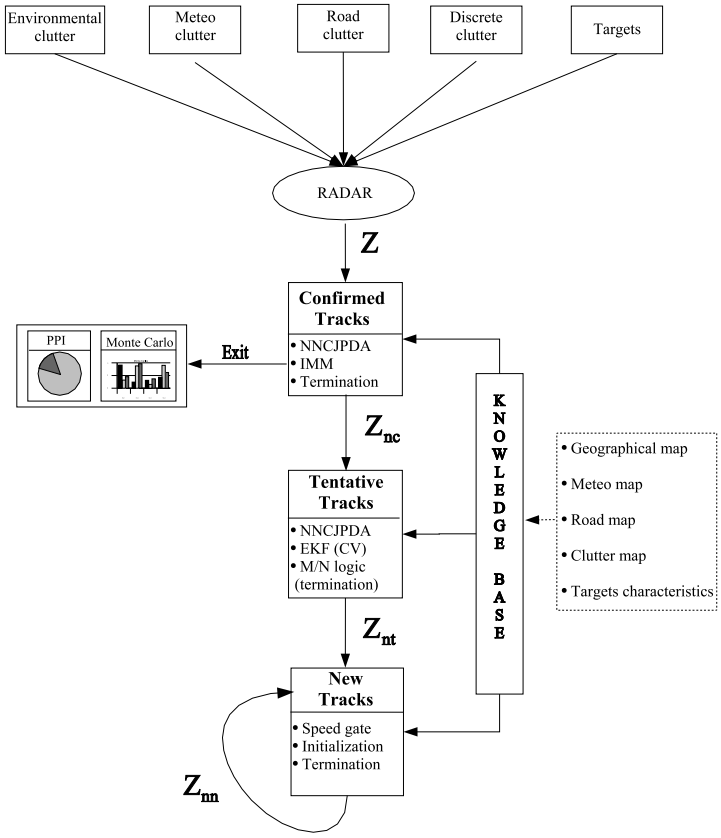

Fig. 3. Architecture of the KB tracking system

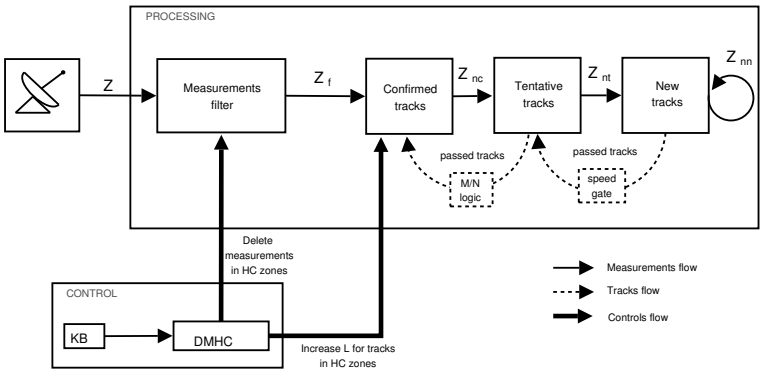

Fig. 4. DMHC strategy

the (estimated) target speed and the (estimated) target location on the maps, are, for instance,

- **if** the target speed is $<$ 40 km/h **and** the target is located on the sea **then** the target is a ship;
- **if** the target speed is $<$ 40 km/h **and** the target is located on the land **then** the target is a helicopter;
- **if** the target speed is $>$ 1200 km/h **then** the target is a military aircraft;
- ...

The above rules are all *memoryless* and are, in most cases, insufficient to classify a target unambiguously. Hence, rules with memory can also be included in the KB such as, for instance,

- **if** the target was a helicopter **and** the target speed is now $<$ 40 km/h **and** the target is in the sea **then** the target is a helicopter;
- **if** the target was an aircraft **and** the target speed is now $< v_e$ km/h **then** the target is an aircraft;

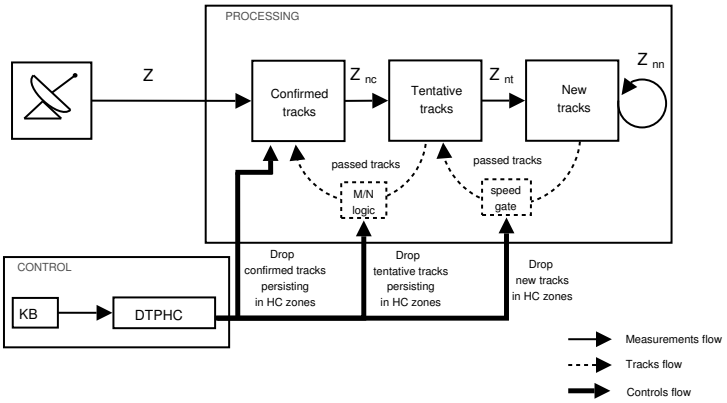

Fig. 5. DTPHC strategy

- ...

where v_e is the maximum speed for a helicopter. The rules with memory must have priority on memoryless rules. Clearly, also the inclusion of rules with memory cannot completely avoid possible ambiguities in target classification; for instance, it does not prevent that a helicopter, never classified as such, flying on the sea can still be classified as a ship. This ambiguity could, for instance, be eliminated using information on the amplitude of the radar echo as will be discussed in the next subsection. Also notice that the ship-helicopter ambiguity is obviously circumvented if the radar also provides elevation measurements, which is not the case considered in this paper.

Once the target has been classified, the information on the target's type can be properly exploited in the various steps of tracking.

- In the **data association** it can, for instance, prevent a track of a ship sailing along the coast from being updated with measurements on the land.
- In the **filtering**, the knowledge of the target's type can suggest modifications to the IMM models such as
  - a change of the parameter ω_0, in the models CT_+ and CT_-, according to the type of target;
  - a change of the model set depending on the type of target [2](e.g., a slowly-maneuvering ship can be effectively tracked using a single CV model instead of the three models CV, CT_+, CT_-).

In summary target classification is improved by the KB (maps and characteristics of the targets) and this, in turn, along with the KB can be used in the data-association and filtering to improve the tracking performance.

E. Amplitude information

The radar echo wave is characterized by a power given by the *radar equation*

$$P_r \;=\; \sigma\; \frac{G_t^2\; G_r^2\; P_t\; \lambda^2\; F_t^2\; F_r^2}{64\; \pi^3\; R^4\; L_{tot}}$$

where: G_t and G_r are the gains of the transmitting and receiving antenna, respectively; λ is the wavelength; σ is the target's *Radar Cross Section (RCS)*; R is the target range; L_{tot} represents the total losses of the radar system; F_t and F_r are the transmitter and receiver propagation factors, respectively; P_t and P_r are the transmitter and received power, respectively. The amplitude of the received signal is $A = \sqrt{2P_r}$. In this way, each measurement provided by the radar is characterized by $[r, \theta, A]$. Given two targets with the same position $[r, \theta]$, the echo's amplitude might differ because of the RCS that depends on the shape, area, orientation and material of the target. Echoes arise not only from the targets of interest but also from clutter; the echo amplitude can be exploited to distinguish the source of the radar echo. A simple way to use such information is to eliminate, in the data association, all measurements that are not characterized by a RCS compatible with the track under examination.

In an urban environment, for instance, there exist clutter measurements having high amplitudes compared to the targets of interest (e.g. aircraft and helicopters). The elimination of such measurements, that are incompatible with the RCS of the targets, clearly reduces the probability of false alarms and, thus, favours the association. The difficulty in applying this strategy is due to the fluctuations of the RCS. In Figure 6 a typical plot of the target echo amplitude vs. target range is reported. This amplitude decays to zero with the range R as $1/R^2$, but exhibits large fluctuations due to target glints, surface multipath effects etc. Figure 6 also displays the ideal (average) amplitude behavior (solid line) and the 80% confidence band (dashed lines). By means of simulation experiments, it has been checked that a precise prior knowledge of the range of the RCS (e.g. 80% confidence band) of a given target allows an effective elimination of the incompatible measurements and, hence, a significant performance improvement. The main problem is, clearly, how to infer information about the range of variation of the RCS. There exist two possible alternatives for the determination of such a range:

- on-line estimation;
- off-line estimation and consequent inclusion in the KB.

The on-line estimation of the RCS of a track is a difficult task, since the RCS is fluctuating randomly and also because clutter measurements can erroneously be used in the estimation. As a consequence, a large number of measurements is required for a reliable on-line estimate of the RCS. Another approach is

to include in the KB the RCS's range for each type of target provided that this has been suitably estimated off-line. In this case, however, the key point for a correct choice of the RCS is a reliable target classification. A possible way to overcome both difficulties is to adopt the following mixed strategy:

1) perform classification in the first few scans in order to establish the target's class;
2) get the RCS's *range* (i.e. the interval of RCS variations) relative to the estimated target's class from the KB;
3) iteratively refine the RCS's range via on-line estimation.

Even a rough target classification can help in eliminating a large number of measurements with out-of-*range* amplitudes.

IV. Performance evaluation

In this section simulation experiments, carried out in a realistic scenario, are discussed in order to demonstrate the superior performance of KBT systems with respect to a *standard* tracking system that does not exploit the KB. To evaluate tracking performance, the following metrics will be adopted:

1) the percentage of successful target tracks;
2) the number of false confirmed tracks;
3) the number of tentative tracks.

These are natural indexes for the performance of a radar tracker, as the main objectives are:

- to maximize the probability of recognizing true tracks;
- to maximize the probability of rejecting false tracks;
- to minimize the number of scans for track initiation.

These objectives are related to the first two metrics, while the third metric is essentially related to the computational load of the tracking algorithm. To make the concepts of true and false tracks more precise, a target of interest is considered *under track* at a given scan if the distance between the true target position and the estimated position does not exceed vT, that represents the maximum distance travelled by that target during a scan period. Hence, at a given scan, all confirmed tracks that either are not associated to true targets or do not satisfy the above distance condition, will be considered as *false tracks*. Further, whenever a confirmed track loses the target, new tracks assigned to the target are not counted as successful target tracks until the original confirmed track is recognized as a false track and terminated. This makes the "percentage of successful target tracks" a good performance metric also for track swaps and track continuity. To better understand this, let us consider a tracking experiment with a single target present for all the duration of the experiment and let us associate to such an experiment a binary sequence defined in this way: at a given scan, 1 means that there is a successful target track while 0 means that there is no successful target track according to the above described logic. Suppose that a confirmed track, say track A, has been tracking the true target up to a given scan k, then loses the target and is terminated after S scans and suppose that another confirmed track, say track B, is tracking the target from scan $k+1$; then we get the following sequence:

$$\cdots 11\underbrace{00\cdots0}_{S}11\cdots$$

The percentage of successful target tracks at each scan is obtained by averaging the above sequences over several Monte Carlo runs. Clearly a track swap induces a sequence of zeros and hence penalizes such a metric. Further, the time-averaged percentage of successful target tracks gives a measure of *track continuity* as it provides the average fraction of time in which the target has been under track. Finally the number of tentative tracks will count only *false tentative* tracks.

The following four trackers will be compared in this section:

- NKB: tracker that does not exploit at all contextual information;
- DMHC: KBT using the DMHC strategy;
- DTPHC: KBT using the DTPHC strategy;
- DTPHC-AI: KBT using the DTPHC strategy and AI.

All the above listed trackers use the M/N logic for track initiation, the NNCJPDA algorithm for data association and the IMM algorithm with three models (CV, CT_+, CT_-) for filtering. Notice that *NKB* represents a standard tracker that does not use the KB. Conversely the other three trackers (DMHC, DTPHC, DTPHC-AI) use the KB in different ways; more precisely, they all adopt zone-dependent parameters (M, N, γ, b) and use respectively the DMHC strategy, the DTPHC strategy and the DTPHC strategy with Amplitude Information.

The trackers have been evaluated on a simulated scenario characterized by live clutter (Figure 2) and by artificial target tracks that have been located on zones of the surveillance environment with different clutter density. Moreover, in the experiments pertaining to the use of Amplitude Information (see section IV-D) also real aircraft tracks have been considered. The live data pertain to a X-band AMS naval radar capable of 2D air and surface surveillance, over the horizon detection, detection of low flying targets, autonomous capability of target velocity estimation via MTD and track while scan. The radar gives accurate measures of plot range and azimuth plus a rough estimate of plot amplitude that have been used for the application described in this work. The utilized data refer to clutter recorded during the internal test of the system. The following case-studies will be examined in detail:

- raft ($P_d = 0.4$) located on the sea surface far from the coast;
- raft ($P_d = 0.4$) located on the sea surface near to the coast;
- aircraft ($P_d = 0.8$) crossing the coastline in a HC zone without maneuver;
- aircraft ($P_d = 0.8$) crossing the coastline in a HC zone with a maneuver.

In all simulations the target's detection has been generated as a random draw with probability P_d. For each of the above listed case-studies, the previously defined trackers have been compared by means of Monte Carlo simulations (60 runs). Monte Carlo simulations have been carried out by varying, trial-by-trial, the clutter plot positions (randomly selected among the recorded radar scans pertaining to live data), the measurement noise and the missed plots for the test target. Table II reports the choice of the various parameters M, N, b, γ, L, L_s used in

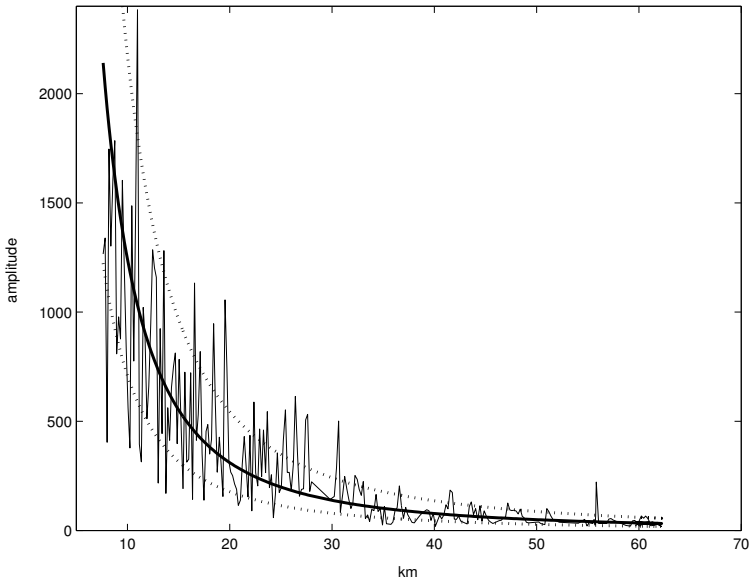

Fig. 6. Typical plot of target echo amplitude vs. target range

TABLE II
PARAMETER VALUES

	NKB						DMHC						DTPHC					
	M	N	b	γ	L	L_s	M	N	b	γ	L	L_s	M	N	b	γ	L	L_s
LC	5	7	10^{-4}	4.6	3	-	3	4	0	9	3	-	3	4	0	9	3	-
MC	5	7	10^{-4}	4.6	3	-	4	7	10^{-5}	6	3	-	4	7	10^{-5}	6	3	-
HC	5	7	10^{-4}	4.6	3	-	-	-	-	-	8	-	6	8	10^{-3}	4.6	3	8

the simulations in the LC, MC, HC zones. The false alarm probability threshold values that define the LC, MC, HC zones according to (13) have been set to $P_{fa}^1 = 10^{-3.5}$ and $P_{fa}^2 = 10^{-2.5}$, via trial-and error so as to get $1-2$ false confirmed tracks per hour. In the two subsequent subsections, for each case-study, the performance of the trackers NKB, DMHC and DTPHC will be compared, while the performance obtained also with the use of amplitude information (DTPHC-AI tracker) will be examined in the last subsection.

A. Raft simulation results

A raft represents a critical target for two reasons:

- it has low detection probability P_d,
- it can be confused with the littoral clutter whenever it navigates in the neighborhood of the shore.

To simulate these characteristics, two types of experiments have been carried out:

1) tracking of a raft far from the shore,
2) tracking of a raft close to the shore.

In these experiments a speed of 35 knots and a detection probability $P_d = 0.4$ have been assumed for the raft. The simulation results relative to the NKB, DMHC and DTPHC trackers are shown in Figures 7 and 8 that display the percentage of successful target tracks vs. time (measured as the number of radar scans starting from scan 0 that refers to the beginning of the simulation). In Figure 7, it can be seen that DMHC and DTPHC are not distinguishable since, far from the coast (in the open sea), there are no HC zones and, hence, there is no difference between the DMHC and DTPHC strategies. The improved performance of DMHC/DTPHC w.r.t. NKB is therefore due only to the different tuning of the parameters, in particular the parameters M and N of the track promotion logic. In fact, for tracking the raft it is appropriate to use low values of the parameter M as this is directly related to the target detection probability P_d. On the other hand, the NKB tracker must work with fixed M and N parameters since, by definition, it is not able to identify the type of zone (LC, MC or HC) and hence to appropriately tune the tracking parameters (M, N, γ, b).

When the raft is sailing near to the coastline (see the results in Figure 8) the situation is more complicated since, besides the missed target detections, there can be frequent association errors due to the littoral clutter. This negative influence of the littoral clutter is mitigated in the KBTs that, thanks to the internal knowledge-based rules, prevents a track, previously attributed to a ship, from being continued on the land. Figure 8 shows that the performance obtained with DMHC and DTPHC in this case (raft nearby the coastline) is almost the same as in the previous case (raft far from the coast, see Figure 7)

B. Aircraft simulation results

Two cases concerning respectively a maneuvering and a non-maneuvering aircraft crossing the coastline over a HC

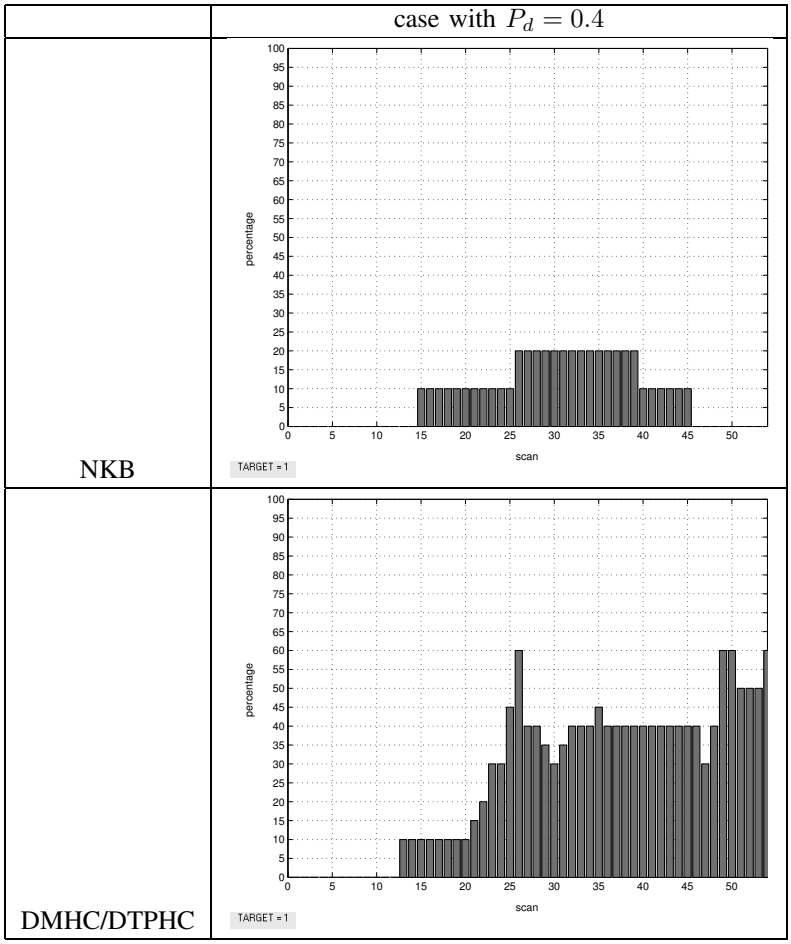

Fig. 7. Raft far from the shore: percentage of successful target tracks

zone have been considered. For the aircraft a speed of $0.3\ km/s$, an angular speed during the maneuver of $0.2\ rad/s$ and a detection probability $P_d = 0.8$ have been assumed. Figure 9 displays the trajectories of the aircraft used in the simulations while Figures 10 and 11 show the results of the simulations for the crossing of the HC zone.
During the crossing the aircraft remains in the HC zone for three scans in the maneuverless case and for six scans in the maneuver case. Moreover, in the case of maneuverless crossing, the aircraft moves across by a LC zone before reaching the HC zone and then proceeds in a MC zone; conversely, in the maneuvering case the aircraft comes from an LC zone before the crossing and then enters again an LC zone.

Looking at the performance of the NKB tracking system (cf. Figures 10 and 11) it can be observed that the track is first detected at scan 6, as expected since a tentative track is promoted after reaching M (in this case $M = 5$) plots. Conversely, for the knowledge-based trackers DMHC and DTPHC, $M = 3$ has been chosen and, in fact, the track is promoted after 4 scans. A closer examination of Figure 10 reveals the difficulty of the standard tracking system NKB even in presence of a transverse crossing of the coastline, since the high concentration of clutter makes the target's loss an event with very high probability. On the other hand, the two KBTs have much higher percentages of successful tracking; in particular DMHC yields a better performance as the cancellation of all clutter measurements falling in the coastal area totally avoids association errors.

The maneuver considered in Figure 9 is a critical one since the target, coming from the sea (LC zone), turns in proximity of the coastline, then proceeds for a while along the coastline and then turns again, so that it finally proceeds in the opposite direction with respect to the original one. Clearly the standard tracker NKB yields the worst performance, for the same reasons as in the maneuverless case (see Figure 11) . The DMHC KBT looses the track as soon as the target enters the HC coastal zone (scan 9), since the shadowing of the coastal zone enforces missed detections that, in the maneuvering case, lead to the target's loss. For the DTPHC tracker, the critical phase is the exit from the coastal HC zone (scan 13) rather than the entry in such a zone. The comparison between DMHC and DTPHC in Figures 10-11 reveals that DMHC (respectively DTPHC) is preferable in the case of a *non maneuvering* (respectively *maneuvering*) target.

C. Number of false tracks and tentative tracks

The proposed knowledge-based strategies have also been evaluated in terms of the numbers of false confirmed tracks and of false tentative tracks due to clutter. Table III reports

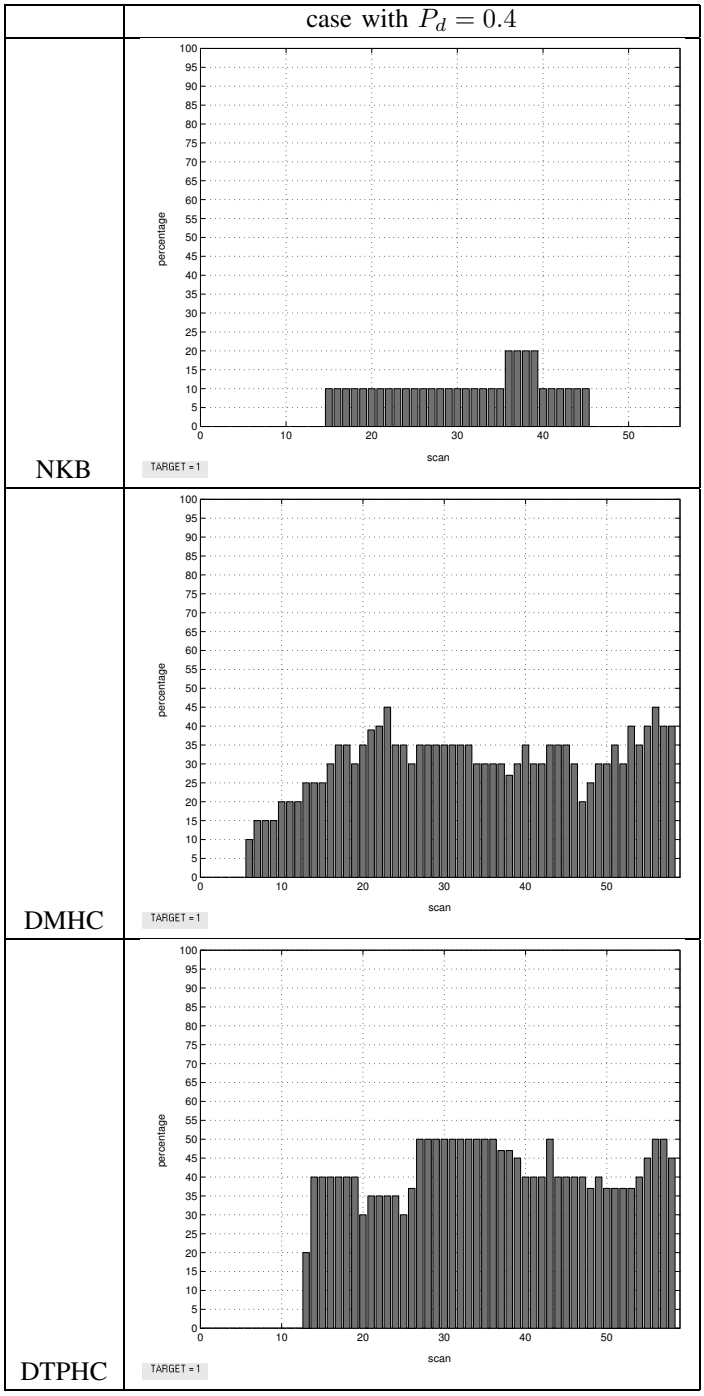

Fig. 8. Raft near to the shore: percentage of successful traget tracks

the average values of such indices. It can be observed that the use of contextual information in the KBTs allows to significantly reduce both the number of false tracks and the number of tentative tracks. In particular the DMHC yields better results, via total elimination of measurements in the HC zones; however, also the DTPHC gives a good performance in successfully recognizing false tracks. From the examination of the simulation results reported in Table III and in Figures 10-11, it can be observed that

- the use of KBTs yields better results, compared to NKB, for all the considered metrics;
- in the maneuverless case, DMHC provides better performance than DTPHC and the converse holds in the maneuvering case;
- DMHC provides a reduced number of false confirmed tracks and of tentative tracks.

Hence, the following conclusions can be drawn.

- In the small-extension HC zones it can be convenient to adopt the DMHC strategy so as to eliminate plots and thus reduce the computational load, since targets cannot perform critical maneuvers inside such zones due to the small extension.

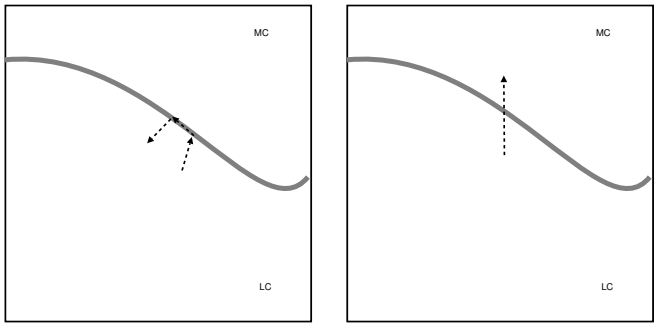

Fig. 9. Aircraft paths

TABLE III
NUMBER OF FALSE CONFIRMED AND TENTATIVE TRACKS

	confirmed false tracks no./hour	tentative tracks no./scan
NKB	2.5	350
DMHC	0.3	200
DTPHC	0.4	250

TABLE IV
PERCENTAGE OF SUCCESSFUL TARGET TRACKS

DTPHC	44%
DTPHC + AI exact	80%
DTPHC + AI (30% error bound)	60%
DTPHC + AI (50% error bound)	48%

- In the large-extension HC zones, the DMHC strategy does not work properly and the DTPHC strategy has to be adopted.

From Figure 11 it can be seen that, in the case in which the target crosses an HC zone with a maneuver, the performance of KBTs, though improved with respect to NKB, is nevertheless unsatisfactory. The use of amplitude information can overcome this problem.

D. The use of amplitude information

Figure 6 shows a typical trend of the target echo amplitude vs. target range, concerning a sample of 240 real data plots. This amplitude decays to zero with the range R as $1/R^2$, but exhibits large fluctuations. Figure 6 also displays the ideal (average) amplitude behavior (solid line) and the 80% confidence band (dashed lines).

In order to evaluate the benefits arising from the use of *amplitude information (AI)*, real data concerning an aircraft that performs a critical maneuver in an HC zone (see Figure 9) have been considered. The real values of the amplitude are reported in Figure 6. The AI, as specified in Section III-E, is employed in the data association in order to eliminate all the (clutter) plots whose amplitude values are incompatible with the target amplitude confidence band of Figure 6. In order to carry out this elimination, it is assumed that the range of the amplitude is a priori given for each type of target. Clearly, the ambiguity in target classification implies an uncertainty on the amplitude interval.

Table IV reports the percentage of successful target tracking (averaged over the time period of HC crossing) obtained for the tracking of the above mentioned target with the following KBTs:

- DTPHC without AI,
- DTPHC with exact knowledge of the confidence band,
- DTPHC with a 30% confidence bound,
- DTPHC with a 50% confidence bound.

In particular the last two cases allow the evaluation of the effect on the performance of the amplitude range uncertainty. From Table IV it can be observed how the performance is significantly improved by a precise knowledge of the amplitude range and how a rough estimate of such a range can still yield benefits. This motivates the approach proposed in Section III-E, that consists of using all measurements associated to the track, scan by scan, in order to iteratively refine the estimate of the amplitude and, thus, increase the effectiveness of the amplitude-based elimination as far as the track's life proceeds.

V. CONCLUSIONS

A *Knowledge-Based (KB)* system for multi-target tracking using a ship-borne radar operating in a complex scenario has been studied. The main ingredients of the tracker are:

- *Extended Kalman filtering* to take into account non linear target and measurement models;
- *Interacting Multiple Model* for managing the target maneuvers;
- *Nearest Neighbor Cheap Joint Probabilistic Data Association* for robust plot-track association;
- *M out of N logic* for track initiation;
- use of the *Knowledge-Base* and of *Amplitude Information*.

The technical solution has been tested against simulated and live data pertaining to an AMS naval surveillance radar and it has been demonstrated that the KB approach provides meaningful advantages allowing the reduction of false and tentative tracks while permitting the continuous track of useful targets. More in detail, the used KB incorporates geographical, clutter, road and meteorological maps as well as a priori information

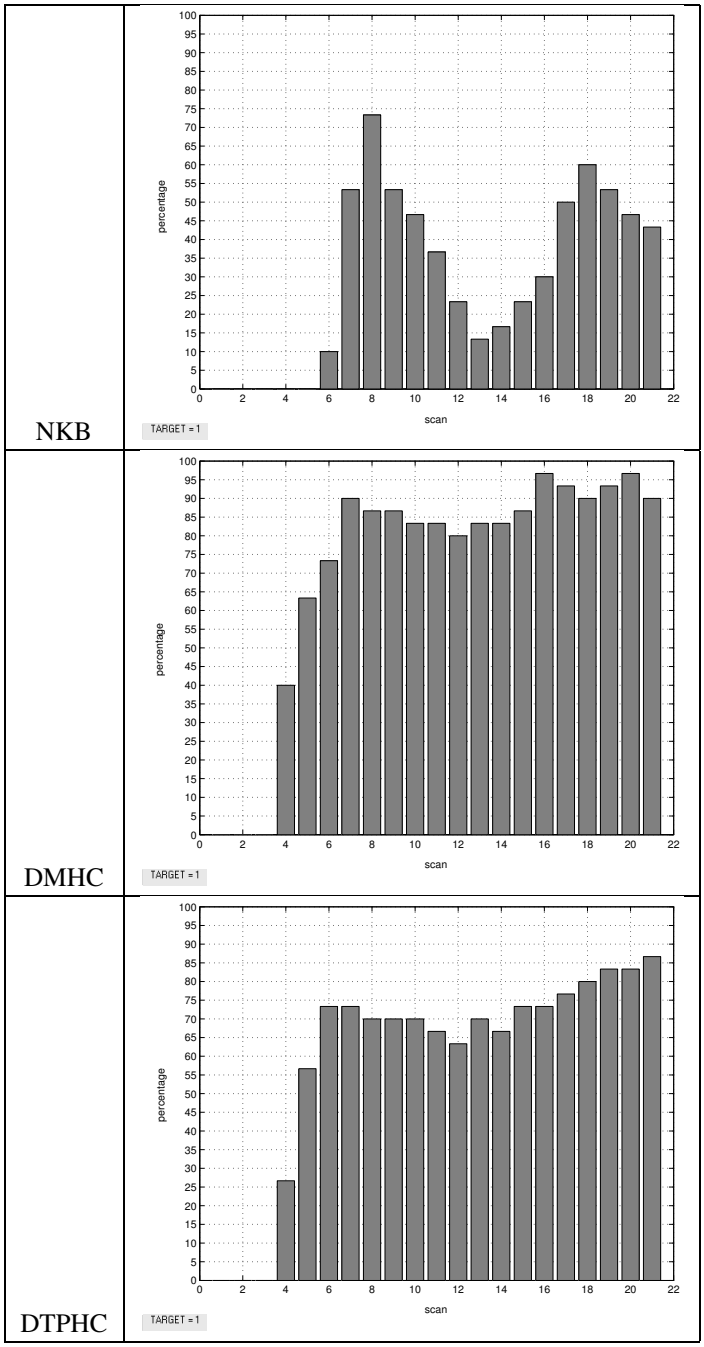

Fig. 10. Aircraft crossing the shore in a HC zone without maneuver: percentage of successful target tracks

on the target characteristics, i.e. maximum velocity and RCS. Future steps to refine the KB tracking system will be:

- the inclusion of statistical models for the echo amplitude of the various sources (e.g. targets and clutter) using the maximum likelihood estimation technique;
- use of the echo amplitude to improve the track initiation logic;
- potential benefits of *Particle Filtering* [17] in lieu of EKF and/or IMM-EKF.

REFERENCES

[1] A. Farina, F.A. Studer, *Radar Data Processing, vol. I: Introduction and Tracking*. John Wiley & Sons, New York, 1985.

[2] Y. X. R. Li, *Engineer's Guide to Variable-Structure Multiple-Model Estimation for Tracking* in Bar-Shalom, Y. (Ed.) *Multitarget-Multisensor Tracking: Applications and Advances.* Volume III, chapter 10, Artech-House, Norwood, MA, 1996.

[3] G.A. Ackerson, K.S. Fu, "On State Estimation in Switching Environments", *IEEE Trans. Automatic Control*, vol. 15, pp. 10-17, 1970.

[4] C.B. Chang, M. Athans, "State Estimation for discrete systems with Switching Parameters", *IEEE Trans. Aerospace and Electronic Systems*, vol. 14, pp. 418-425, 1978.

[5] H.A.P. Blom, Y. Bar-Shalom, "The interacting Multiple Model Algorithm for Systems with Markovian Switching Coefficients", *IEEE Trans. Automatic Control*, vol. 6, pp. 473-483, 1970.

[6] R.A. Singer, "Estimating Optimal Tracking Filter Performance for Manned Maneuvering Targets", *IEEE Trans. Aerospace and Electronic Systems*, vol. 15, pp. 10-17, 1970.

[7] Y. Bar-Shalom, X.R.Li, *Multitarget-Multisensor Tracking: Principles*

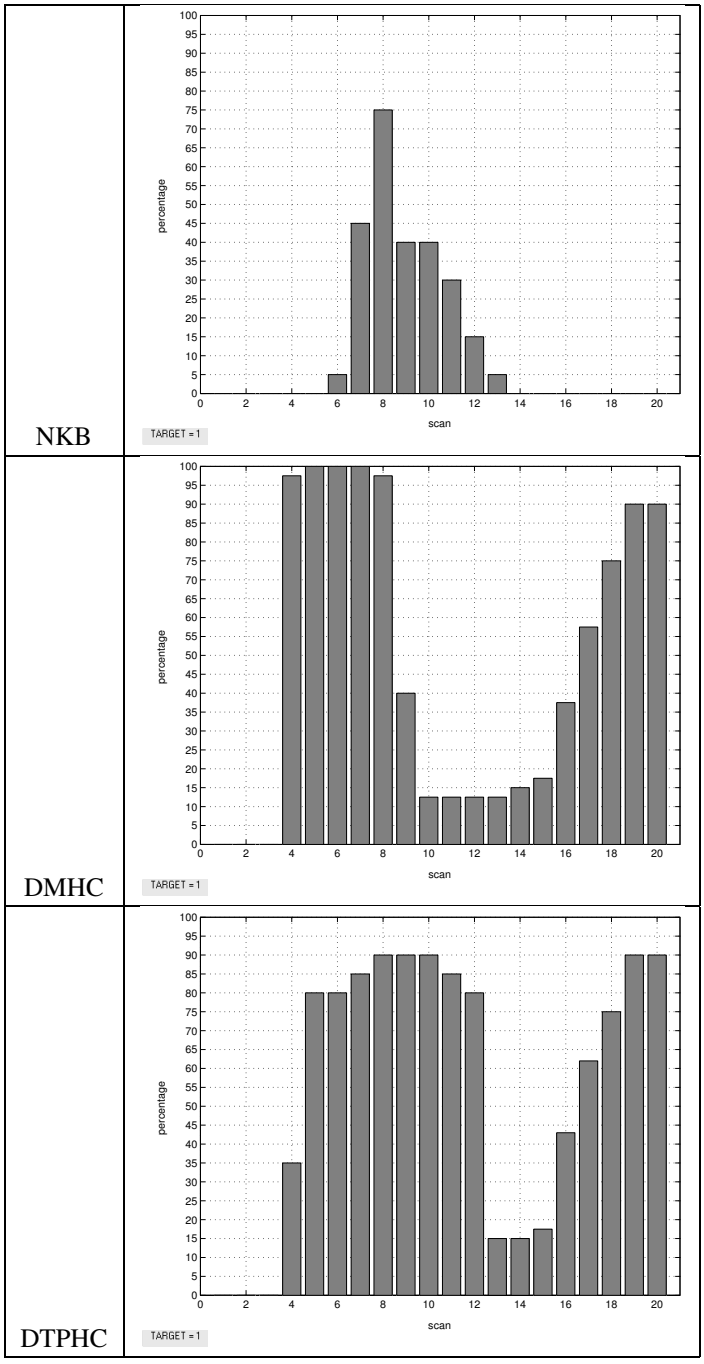

Fig. 11. Aircraft crossing the shore in a HC zone with maneuver: percentage of successful target tracks

and Techniques. YBS Publishing, Storrs, CT, 1995.

[8] Y. Bar-Shalom, X.R.Li, T. Kirubarajan, *Estimation with Applications to Tracking and Navigation.* John Wiley & Sons, New York, 2001.

[9] Y. Bar-Shalom, *Multitarget-Multisensor Tracking: Advanced Applications.* Volume I, Artech-House, Norwood, MA, 1990.

[10] T. E. Fortmann, Y. Bar-Shalom, M. Scheffe, "Sonar Tracking of Multiple Targets Using Joint Probabilistic Data Association", *IEEE Journal Oceanic Engineering*, vol. 8, pp. 173-184, 1983.

[11] A. Farina, M. De Feo, A. Graziano, R. Miglioli, "IMMJPDA versus MHT and Kalman filter with NN correlation: performance comparison", *IEEE Proc. - Radar, Sonar Navigation*, vol. 144, pp. 49-56, 1997.

[12] R. Torelli, A. Graziano, A. Farina, "IM3HT algorithm: a joint formulation of IMM and MHT for multitarget tracking", *European Journal of Control*, vol. 5, pp. 46-53, 1999.

[13] D. Reid, "An algorithm for tracking Multiple Targets", *IEEE Trans. Automatic Control*, vol. 24, pp. 843-854, 1979.

[14] F. R. Castella, "Sliding Window Detection Probabilities", *IEEE Trans. Aerospace and Electronic Systems*, vol. 12, pp. 815-819, 1976.

[15] A. Farina, "Application of Knowledge-Based Techniques to Tracking Function", *NATO RTO Lecture Series 233*, Neully Sur Seine Cedex, France, 2003.

[16] C. Morgan, L. Moyer, "Knowledge-based applications to adaptive space-time processing. Volume V: Knowledge-based tracking rule book", AFRL-SN-TR-2001-146 Vol. V (of Vol. VI), Final Technical Report, 2001.

[17] B. Ristic, S. Arulampalam, N. Gordon, *Beyond the Kalman filter: particle filters for tracking applications*, Artech House, Norwood, MA, 2004.